

**1\* Nurul Huda Abdul Razak**

**2\* Badariah Bais**

**3 Nowshad Amin**

**4 Kamaruzzaman Sopian**

**5 Md. Akhtaruzzaman**

## Optimizing Monofacial Silicon Solar Cells Efficiency Using PC1D Simulation



**Abstract:** - Researchers use computer modelling methods before making the actual solar cells to make sure they use the most solar energy possible. In this study, the Personal Computer One Dimensional (PC1D) computer simulation was used to numerically investigate the values of the input variables that maximize or minimize the output value of a silicon solar cells. The study focused on examining the doping levels and thicknesses of the substrate material, emitter, back surface field (BSF), and antireflection coating (ARC) layers. Based on the simulation results, the optimal thickness for a  $1.513 \times 10^{16} \text{ cm}^{-3}$  silicon p-type substrate is  $200 \mu\text{m}$ . Similarly, for an n-type emitter layer doping concentration, it is  $1 \times 10^{19} \text{ cm}^{-3}$  with a  $0.5 \mu\text{m}$  thick, and for a BSF layer doping concentration, it is  $1 \times 10^{18} \text{ cm}^{-3}$  with a  $1 \mu\text{m}$  thick, at a  $3 \mu\text{m}$  pyramid height and an angle of  $54.74^\circ$ . Starting with a single layer of titanium dioxide ( $\text{TiO}_2$ ) with a thickness of  $67 \text{ nm}$  and a refractive index of  $2.116$ , a simulation was conducted to optimize the effective parameters, and the results demonstrated a  $22.98\%$  efficiency in the solar cells. According to the simulation, a  $10 \text{ cm}^2 \times 10 \text{ cm}^2$  p-type monocrystalline silicon wafer with a thickness of  $200 \mu\text{m}$  can boost solar cell efficiency to  $24.51\%$  when triple-layer antireflective coatings (TLARC) are applied. It seems that antireflection coatings (ARC) reduce reflection, increasing the solar cell's efficiency from  $16.06\%$  to  $24.51\%$  on the textured surface.

**Keywords:** Monocrystalline silicon solar cells, PC1D, Thickness, Doping concentration, Antireflection coating, and, Efficiency

### I. INTRODUCTION

Solar radiation, also referred to as the solar constant is one of renewable energy which has an average value of  $1361\text{-}1362 \text{ W/m}^2$  and has the potential to produce a huge amount of energy, which is sufficient to meet all of humanity's energy requirements, both now and in the future. With adequate sun irradiation, this energy can be transformed into useful electrical energy during the day by using solar panels or photovoltaic (PV) systems [1]. For the first time, renewable energy sources have surpassed coal as the primary source of electricity generation capacity worldwide. About  $30\%$  of the world's electricity comes from solar cells. Solar cells, or photovoltaic devices, are one of the most effective techniques for harnessing sunlight-absorbing photons and converting light energy into electrical energy through the photovoltaic effect. Solar cells are usually made using the most common semiconductor which is silicon because silicon is one of the most abundant materials on Earth, is cheaper, has a long lifetime, and demonstrates high efficiency. According to a photovoltaic report, the global market share of the solar cell industry is  $97\%$ , dominated by monocrystalline silicon (c-Si) solar cells in c-Si production [2]. As of now, the highest confirmed efficiency for monocrystalline and multicrystalline silicon solar cells is  $15\% \sim 20\%$  [3] and  $15\% \sim 18\%$  [4], respectively.

<sup>1\*</sup>Corresponding author: Department of Electrical, Electronic and Systems Engineering, Universiti Kebangsaan Malaysia, Bangi 43600, Selangor, Malaysia; Email: p90615@siswa.ukm.edu.my

<sup>2\*</sup>Corresponding author: Department of Electrical, Electronic and Systems Engineering, Universiti Kebangsaan Malaysia, Bangi 43600, Selangor, Malaysia; Email: badariah@ukm.edu.my

<sup>3</sup> Department of Electrical and Electronic Engineering, Faculty of Engineering, American International University-Bangladesh (AIUB), 408/1 Kuratoli Road, Kuril, 1229 Dhaka, Bangladesh

<sup>4</sup> Department of Mechanical Engineering, Universiti Teknologi PETRONAS, 32610 Seri Iskandar, Perak Darul Ridzuan, Malaysia

<sup>5</sup> Department of Chemistry, Faculty of Science, Islamic University of Madinah (IUM), 42351 Madinah, Saudi Arabia

Silicon in crystalline form is called crystalline silicon (c-Si) which is made up of silicon atoms arranged in a diamond cubic crystal lattice structure [5-6]. The lattice's organized structure improves light-to-electricity conversion efficiency. The structure of a silicon cell resembles a sandwich with four separate pieces. The bread on both sides is made of thin strips of metal that serve as electrodes. The power produced by the solar cells is extracted and transferred to an external circuit. Like a sandwich, the most interesting component is the filling-here where solar photons are transformed into useful electricity. The two layers that fill a solar cell are silicon doped with phosphorus (also called n-type silicon) and silicon doped with boron (sometimes called p-type silicon) [7-9].

A thorough understanding of the basic principles of semiconductor operation is necessary to further improve solar cell efficiency. Using accurate simulation software can help understand how changing the physical and electrical properties of materials affects device performance. With simulation tools, researchers can guess how the device will work with different material properties, like the thickness of the layers, the amount of doping, and so on. Additionally, the simulation tools also incorporate both experimental and mathematical data to predict a solar cell's output performance. There are numerous simulation software available for solar cells, including TCAD (Silvaco and Sentaurus) [10], Quokka [11], SolarEye [12], Griddler [13], AFORS-HET [14], and Personal Computer One Dimensional (PC1D) [15]. However, most of them are expensive, which is a major disadvantage. Alternatively, The University of North South Wales (UNSW) is currently offering PC1D for free. This program was developed by researchers from the Photovoltaics Special Research Centre at the University of Sydney in New South Wales, Australia, a world-renowned solar cell research institution. Since it was introduced until now, PC1D has been the most popular commercially available solar cell simulation software. Numerous organizations and educational institutions, including Australia's University of New South Wales, rely on this program to make models of solar cells. Several researchers employed PC1D to simulate a variety of solar cell types before conducting experiments to confirm the possibility of their projects. For example, Meenakshi et al. simulated multi-junction solar cells [16] while Chowdhury et al. employed PC1D to simulate bifacial solar cells [17]. Other researchers, Belarbi et al. and Chuan et al. also investigated silicon solar cells using PC1D (18-19). With this method, one-dimensional (axial symmetry) simulations of semiconductor-based photovoltaic systems can be performed. Several parameters in PC1D can be adjusted to understand their impact on the device's overall performance, including thickness, resistance, doping levels, recombination, carrier lifetime, and others. PC1D can also provide results in a graphical format, such as Power-Voltage (P-V) characteristics, Current-Voltage (I-V) characteristics, quantum efficiency (QE), and more. These results can be looked at and taken into account when planning how to make a real device. Fortunately, there was proof that the simulation software was nearly accurate and reliable using a market or experimentally made solar cell [20].

In this paper, the effects of critical parameters on the performance of monocrystalline silicon solar cells were investigated. These parameters included substrate material thickness, doping levels, emitter thickness, back surface field (BSF) thickness, and antireflection coating layer. PC1D version 5.9 was utilized to manipulate device parameters to simulate and analyze performance. The outcome highlights the significance of examining and determining the ideal value for every parameter to achieve the highest level of device efficiency. The most impressive aspect of this work is that the optimized parameters of the simulated device were validated by comparing the results to those of a solar cell manufactured on an industrial scale that had the same physical and electrical specifications.

## II. METHODOLOGY

Fig. 1 shows the most common structure of a silicon solar cell used in industry. To achieve high conversion efficiencies, understanding the effect of each layer's different physical and electrical properties is vital. PC1D simulation software was utilized to evaluate the impact of device characteristics on each layer and optimize conversion efficiency.

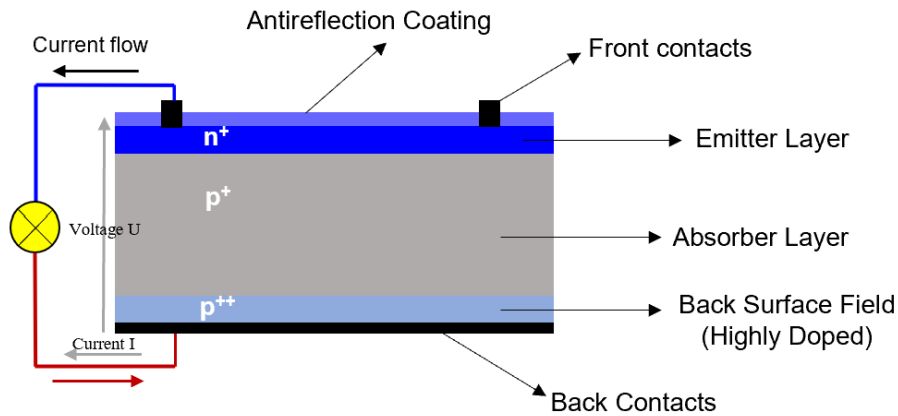


**Figure 1:** The basic structure of a standard silicon solar cell (Monofacial silicon solar cell)

The PC1D version 5.9 has been employed to simulate an energy-efficient monocrystalline silicon solar cell. The simulation also shows the range and effects of texturing, antireflection layer, doping concentration, and diffusion length, as depicted in Fig. 2. This software tool has performed the semiconductor equation, the carrier continuity equation, the Poisson equation, and carrier transport equations, among others. Solar cell device simulations utilizing crystalline Si (c-Si) are performed in the PC1D simulation tool with the help of numerical equations that depict the quasi-one-dimensional flow of electrons and holes in semiconductors. According to Hashmi et. al [21], we can precisely predict how to optimize the properties of the ARC coating layer and other process factors by using PC1D equations to simulate a silicon cell.

PC1D also provides library files containing the properties of crystalline semiconductors used in photovoltaic technology, such as aluminium gallium arsenide (AlGaAs), gallium arsenide (GaAs), germanium (Ge), indium phosphide (InP) and silicon (Si). Furthermore, this software provides access to the solar spectrum files, specifically the AM0 and AM1.5 spectrum. In PC1D, the main window looks like this:

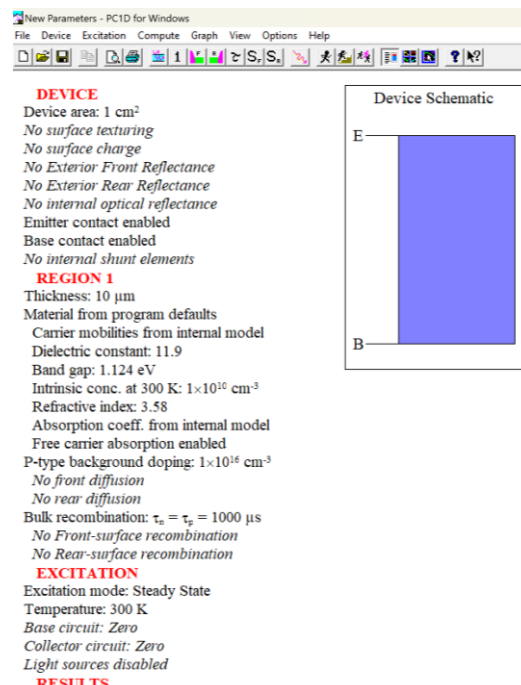


**Figure 2:** PC1D's main window

For accurate and efficient modeling, all of the solar cell's parameters must be included. However, some parameters, like texture and antireflection coating, are not considered at first to keep things simple and help researchers understand how the parameters affect the solar cell model. These are the five most important aspects of PC1D that must be considered:

- i. The part called "Device" has general details about the thing we want to simulate;
- ii. Second-part "Region": This part provides the important details for the component device region, like the materials used, the width, the type of doping, and so on. While the figure above depicts a single area, additional regions can be added (up to a maximum of five regions are possible), or removed (a minimum of one region is required);
- iii. The "Device schematic" part is just a plan of the thing we're making. For example, the colour can change based on the doping, and it can change immediately as soon as one deal with the parameters of the regions.
- iv. The part called "Excitation": this is where we set the parameters of our device's excitation, which will help us model how it would perform. Here we will determine the irradiance, operating temperature, and other factors, for instance, in terms of solar cells;
- v. The "Results" section: This section will contain, in particular, the values of short circuit current ( $I_{sc}$ ), the open circuit voltage ( $V_{oc}$ ), and maximum power voltage ( $V_{pmax}$ ) for solar cell simulation when the simulation is launched;

In this paper, for simulating solar cells, a p-type monocrystalline silicon substrate is taken into consideration, and the device area of a solar cell is set to  $10 \text{ cm}^2 \times 10 \text{ cm}^2$ . A device area of  $10 \text{ cm}^2$  could be a good starting point for initial simulations due to its simplicity and ease of calculation for exploring basic device characteristics or conducting preliminary studies. The front reflectance is set to 1000 nm with outer thickness index = 1 (refractive index of air). This way we are setting up a silicon solar cell without antireflection coating.

Hashmi et. al also reported that the textured surface decreases reflection and improves the efficiency of the solar cell by at least 1–2% [21]. In the PC1D simulation, the front surface texture depth of  $3 \mu\text{m}$  with an angle  $54.74^\circ$  is generally considered a good choice for achieving high efficiency [22-25]. This depth is typically selected to optimize light trapping within the cell, reducing reflection and enhancing photon absorption. However, the optimal depth can depend on specific cell designs, material properties, and desired wavelength ranges for efficiency enhancement. While for the angle of  $54.74^\circ$  also corresponds to the critical angle and is significant in optics because it represents the angle at which light refracts through a medium without bending which is defined by Snell's law of refraction.

An exterior front reflectance of 10% is still within an acceptable range as an effective front reflectance value in monocrystalline p-type solar cells. Some researchers discuss optimizing antireflection coatings, including SiN, for silicon solar cells and they explore various thicknesses and refractive indices of SiN to achieve low reflectance values. While specific numbers can vary, they emphasize achieving reflectance levels around 10% or lower as optimal for enhancing solar cell efficiency [26-27]. While lower reflectance values (closer to 4% to 5%) are often targeted for optimal performance, a reflectance of 10% is still within a reasonable range and can be used to assess the solar cell's performance and efficiency under different conditions. It's important to note that actual performance in real-world applications may vary, and further optimization might be required based on specific design goals and conditions.

For monocrystalline silicon p-type solar cells, the internal series resistance at the emitter contact setting is set to  $1 \times 10^{-6}$ . Emitter contact can start from lower values such as around  $10^{-5}$  and high value  $10^{-7}$ . However, this study chose an emitter contact resistance of  $1 \times 10^{-6} \Omega \cdot \text{cm}^2$  which is considered very good for monocrystalline solar cells. The value of  $1 \times 10^{-6}$  represents a balance between achieving reasonably low resistance and optimizing manufacturing costs. It also signifies efficient charge carrier collection and transfer, leading to improved energy conversion efficiency and overall performance of the solar cell. The increased emitter series resistance is compensated by a lower contact resistance, so no loss in the fill factor (FF) occurs [28]. In general, commercial crystalline silicon solar cells must have a lower series resistance value to obtain a higher power conversion efficiency and a better fill factor (FF) [29].

The internal series resistance at base contact can be  $0.04 \Omega$  and  $0.015 \Omega$  for high-efficiency monocrystalline solar cells. However, the lower value of  $0.015 \Omega$  is generally considered better [30-31]. The  $0.015 \Omega$  base contact resistance has a few advantages such as lower resistance implies less voltage drop and reduced power losses across the contact, and enhances the efficiency of charge carrier collection and transport within the solar cell, typically

achieved through advanced metallization techniques and precise manufacturing processes. Consequently, it improves the fill factor and overall efficiency of the solar cell and supports higher current output and better performance under varying light conditions [32].

For ideal shunt resistance, their values typically range from 1,000  $\Omega$  (1 k $\Omega$ ) to 10,000  $\Omega$  (10 k $\Omega$ ) or higher. Achieving such high shunt resistance is crucial for minimizing leakage currents, improving efficiency, and ensuring the optimal performance of the solar cells. A low shunt resistance in high-efficiency monocrystalline p-type solar cells leads to increased leakage currents, reduced voltage output, and overall lower performance and efficiency of the solar cell. Therefore, maintaining a sufficiently high shunt resistance is crucial for optimizing the performance and longevity of solar cells in photovoltaic applications. Still, having a higher shunt resistance in monocrystalline p-type solar cells typically does not damage the cells themselves and higher shunt resistance is generally desirable for solar cell performance [33]. In PC1D shunt resistance parameters, the value of S (Siemens) is used. For example, 0.01 S (Siemens) is equivalent to  $1/0.01 \Omega$ , which is 100  $\Omega$ . A photovoltaic (PV) manufacturer might specify a shunt resistance of 1,000  $\Omega$  (1 k $\Omega$ ) for a particular monocrystalline p-type solar cell product. Another manufacturer might specify a higher shunt resistance of 5,000  $\Omega$  (5 k $\Omega$ ) or 0.0002 S for their premium-grade monocrystalline p-type solar cells. Here, a shunt resistance of 5,000  $\Omega$  for monocrystalline silicon p-type solar cells is indeed very good. It indicates that the cell is likely to have high efficiency, low leakage currents, a good fill factor, and a higher open-circuit voltage, all of which contribute to better overall performance.

Notably, high-efficiency p-type monocrystalline silicon solar cells with a thickness of 150 to 200 micrometers ( $\mu\text{m}$ ) are currently available in the market, and many researchers reported that their ideal silicon wafer thickness ranges from 150 to 200 micrometers ( $\mu\text{m}$ ) [34-37]. This thickness range is standard for many commercially produced high-efficiency solar cells.

This range of 150 to 200 micrometers ( $\mu\text{m}$ ), balances several key factors:

- i. **Light Absorption:** Silicon's absorption coefficient is sufficient to capture most of the usable sunlight within this thickness, ensuring efficient conversion of light to electricity.
- ii. **Mechanical Stability:** Thicker wafers provide better mechanical stability, which is crucial during the manufacturing process to prevent breakage.
- iii. **Cost Efficiency:** Thinner wafers reduce material costs, but there is a trade-off with increased handling challenges and potential efficiency losses due to reduced absorption and increased recombination effects at very low thicknesses.
- iv. **Electrical Performance:** This thickness range minimizes recombination losses and maintains good electrical performance by ensuring that the charge carriers can be effectively collected before they recombine.

Advances in manufacturing and material science have allowed solar manufacturers to optimize cell thickness to this range to balance efficiency, cost, and mechanical stability. These solar cells are widely used in residential, commercial, and industrial solar installations, providing reliable and efficient energy conversion. So, 200 micrometers ( $\mu\text{m}$ ) are used in this study as it is widely cited and commonly used thickness for high-efficiency p-type monocrystalline silicon solar cells due to balancing efficiency, mechanical stability, and cost-effectiveness [38-41].

The ideal background doping concentration for p-type monocrystalline silicon wafers typically ranges between  $1 \times 10^{15}$  to  $1 \times 10^{16} \text{ cm}^{-3}$  [42]. This doping level is chosen to balance various factors such as electrical conductivity, minority carrier lifetime, and overall wafer performance in photovoltaic applications. A common doping concentration for p-type silicon wafers used in solar cells is around  $1 \times 10^{16} \text{ cm}^{-3}$ . This concentration ensures good electrical conductivity while maintaining a reasonable minority carrier lifetime, which is critical for solar cell efficiency. Here,  $1.513 \times 10^{16} \text{ cm}^{-3}$  falls comfortably within this range with the automatic resistivity value of PC1D at 25°C and room temperature.

For a monocrystalline p-type silicon wafer substrate doping concentration is around  $1 \times 10^{16} \text{ cm}^{-3}$  (as used in solar cells), but the ideal doping concentration for the emitter layer (typically n-type) should be significantly higher than substrate doping concentration, and also p-type BSF layer to create a strong p-n junction. In shallower emitters, efficiency is higher, but due to increased sheet resistance, more doping is required to reduce power loss. Thus,

maximum efficiency in shallower emitters is achieved at higher doping concentrations [43]. The typical emitter doping concentration is in the range of  $1,018$  to  $1,020$  atoms per cubic centimeter (cm). The value of  $1 \times 10^{19} \text{ cm}^{-3}$  with  $0.5 \text{ }\mu\text{m}$  is chosen because this concentration ensures a strong electric field at the junction, low contact resistance, and efficient charge carrier separation. This ideal emitter layer thickness can maximize carrier collection efficiency, minimize surface recombination losses, and ensure adequate optical transmission. A research study conducted by Lu et. al shows that an emitter thickness of  $0.5$  to  $1 \text{ }\mu\text{m}$  with a doping concentration of  $1 \times 10^{19} \text{ cm}^{-3}$  is effective for achieving high efficiency while minimizing recombination [44-45].

The back surface field (BSF) layer is an additional layer designed to improve cell efficiency by reducing recombination at the rear surface and reflecting minority carriers (electrons) into the cell. The BSF layer is typically more heavily doped than the base layer to create a strong electric field that repels minority carriers, typically in the range of  $1 \times 10^{18}$  to  $1 \times 10^{19} \text{ cm}^{-3}$  [46]. To reduce carrier recombination and improve overall efficiency, it is recommended that the BSF layer have a thickness ranging from  $1.0$  to  $2.0 \text{ }\mu\text{m}$ . This will ensure that the BSF layer successfully provides a strong electric field at the back surface of the solar cell. It also balances between effective carrier collection and optical considerations within the solar cell design. Other researchers indicate that a BSF thickness of  $1.0$  to  $2.0 \text{ }\mu\text{m}$  is the best value for p-type silicon solar cells [47-48]. In this study,  $1 \times 10^{18} \text{ cm}^{-3}$  with  $1 \text{ }\mu\text{m}$  is chosen.

At the beginning of this study, antireflection coating (ARC) was not employed to observe its effects. The concentration of doping levels ( $\text{cm}^{-3}$ ) ranges from low to moderate to heavy doping concentration. In some circumstances, a larger base voltage range (such as  $-0.8 \text{ V}$  to  $0.8 \text{ V}$ ) could provide for greater design and optimization freedom and higher  $V_{oc}$ . The condition of AM (Air Mass)  $-1.5 \text{ G}$  was chosen to simulate the sun. The number of time steps was set to 16 times to see the time progression. After the simulation, the solar cell's efficiency is observed to be  $16.06\%$  without an antireflection coating layer.

The solar cell's shunt resistance ( $R_{SH}$ ) and series resistance ( $R_S$ ) between the Emitter E and Base B are clearly illustrated in Fig. 3. The parameters used in this study are listed in Table 1.

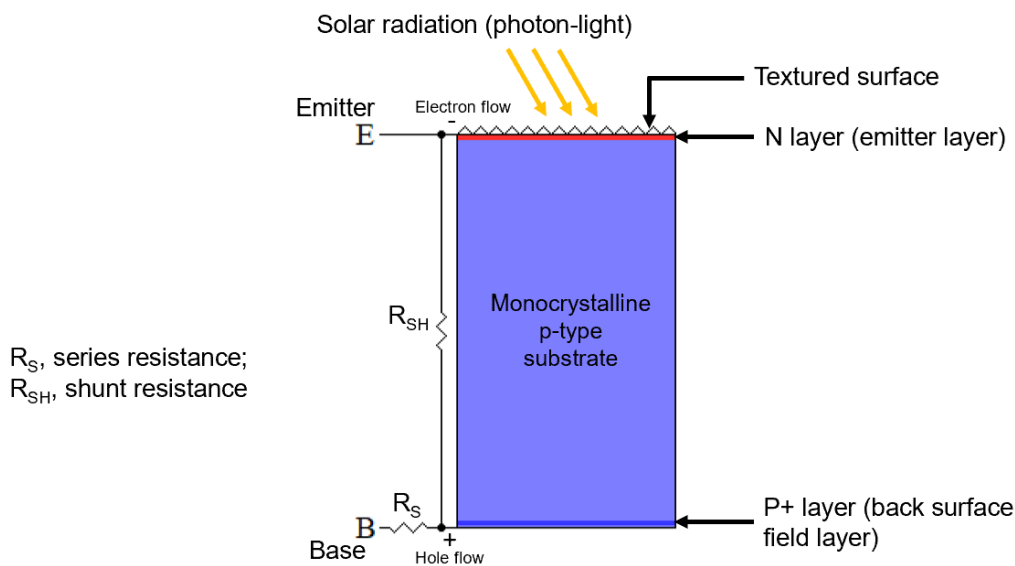


Figure 3: The device schematic of silicon solar cells in PC1D software

Table 1: Parameters of the general testing conditions

Parameters	Value and Unit
<b>Device</b>	
Device area	$10 \text{ cm}^2$
Front surface texture depth	Depth = $3 \mu\text{m}$ , Angle = $54.74^\circ$
Exterior front reflectance	$10\%$
Emitter contact	$1 \times 10^{-6} \Omega$

Base contact	0.015 $\Omega$
Internal conductor/ shunt elements	0.0002 S
<b>Region 1</b>	
Thickness	200 $\mu\text{m}$
Material	Silicon (Si)
Dielectric constant	11.9
Bandgap	1.124 eV
Intrinsic concentration	$1 \times 10^{10} \text{ cm}^{-3}$
P-type background doping	$1.513 \times 10^{16} \text{ cm}^{-3}$
First front diffusion (N-type)	$1 \times 10^{19} \text{ cm}^{-3}$
Bulk recombination	7.208 $\mu\text{s}$
Front surface recombination	$1 \times 10^6 \text{ cm/s}$
Rear surface recombination	$1 \times 10^5 \text{ cm/s}$
<b>Excitation</b>	
Temperature	25°
Base circuit	-0.8 to 0.8 V
Spectrum	AM 1.5G

### III. RESULTS AND DISCUSSION

#### A. Effects of Absorber Layer Thickness on Solar Cell Performance

To determine whether it is feasible to manufacture a photovoltaic device, the cost of semiconductor materials is an important consideration [14]. Selecting materials with the ideal thickness with care is crucial to reducing costs and optimizing device performance. To minimize expenses while maximizing device effectiveness, it is vital to carefully pick substrate materials with the right thickness. The substrate material thickness functions to absorb light and produces mobile charge carriers, which are then carried to and gathered by the contacts to produce electricity. It is also responsible for the absorption of light and the generation of mobile charge carriers. These charge carriers are then transferred to the contacts and collected by them to generate energy [15]. To be noted, greater efficiency is not correlated with a thicker absorber layer because of the way that Voc and short-circuit current density (Jsc) interact. In this section, a solar cell with different absorber layer thicknesses was examined. Table 2 displays how the device's performance is affected by different silicon bulk thicknesses. In Fig. 4, we can observe how the thickness of the absorber layer influences Voc, Isc, and efficiency in Fig. 5.

**Table 2:** Parameters of the general testing conditions

Thickness, $\mu\text{m}$	Short-circuit current (Isc), A	Maximum power output (Pmax), W	Open-circuit voltage (Voc), V	Fill Factor (FF)	Efficiency (%)
30	0.2432	0.1503	0.7296	0.8471	15.03
50	0.2512	0.1539	0.7275	0.8421	15.39
70	0.2557	0.1558	0.7253	0.8401	15.58
90	0.2587	0.1576	0.7273	0.8376	15.76
110	0.261	0.1587	0.7212	0.8431	15.87
130	0.2627	0.1594	0.7192	0.8437	15.94
150	0.2642	0.1599	0.7174	0.8436	15.99
170	0.2654	0.1603	0.7157	0.8439	16.03
190	0.2664	0.1605	0.7141	0.8437	16.05
210	0.2673	0.1606	0.7125	0.8433	16.06
230	0.268	0.1607	0.711	0.8434	16.07
250	0.2687	0.1607	0.7096	0.8428	16.07

300	0.2701	0.1607	0.7064	0.8422	16.07
350	0.2712	0.1605	0.7034	0.8414	16.05
400	0.2721	0.1603	0.7008	0.8406	16.03
500	0.2734	0.1597	0.6962	0.839	15.97

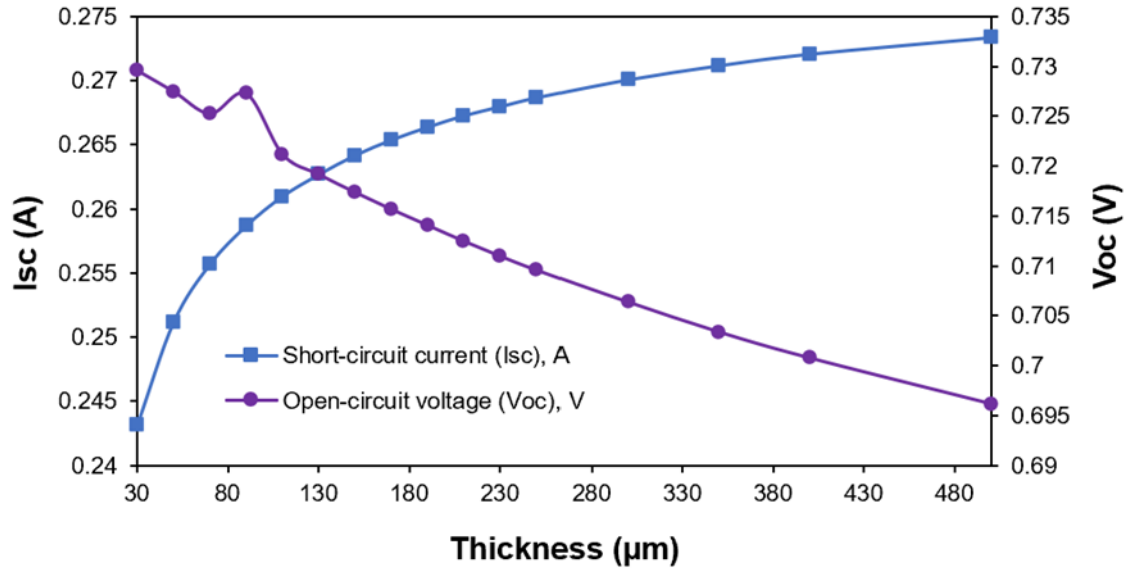


Figure 4: Effects of substrate layer thickness on Isc and Voc

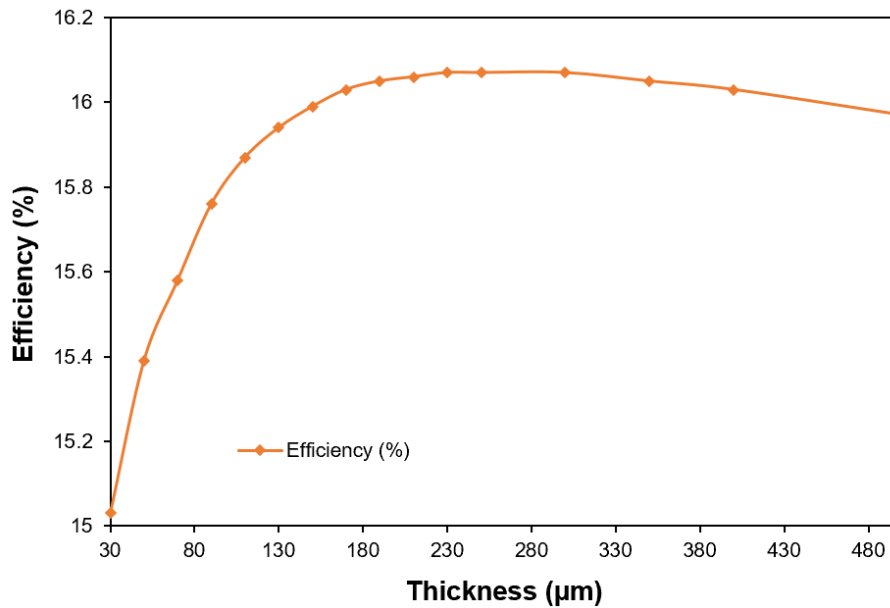


Figure 5: Effects of substrate layer thickness on the efficiency of solar cells

As the thickness of the substrate increases from 30 to 500 μm, the Voc value decreases while the Isc value increases till 500 μm is reached. With increasing thickness above 300 μm, the overall efficiency of the device gradually decreases. Although the 30 μm thick device is started at good efficiency, manufacturers typically make for devices with thicknesses more than 150 μm because of physical limitations, such as the bowing effect of the usual aluminum back surface field, and the difficulties in handling such a tiny device. The production methods should also take into account properties like stability, longevity, and the ability to withstand severe weather. Although silicon has a thickness of 100-200 μm and is often brittle, it can absorb up to 20% of the visible and near-infrared light due to its indirect band gap. However, traditional Si-based solar cells need crystalline silicon materials with a thickness of

more than 200  $\mu\text{m}$  to fully absorb sunlight, which causes the high cost of Si-based solar cells [49-50]. Today, at 200  $\mu\text{m}$ , the substrate is considered thick enough to absorb a large amount of the incoming solar radiation. Because the bulk of the produced carriers are far from the surfaces where recombination rates usually are higher, a thickness of 200  $\mu\text{m}$  helps to minimize surface recombination losses. This improves total carrier collection efficiency.

### B. Effects of Emitter Doping Concentration and Thickness on Device Performance

Generally, when a solar cell's surface absorbs a large amount of light, the generation rate is high. However, when there is a lot of doping in these layers, light doesn't pass through as well, and there is a higher rate of recombination [17]. To absorb the majority of incoming light, the doping concentration and emitter thickness need to be carefully considered. In addition, there needs to be a high concentration to help the drift transport process work better and lower the sheet resistance. Therefore, the ideal doping concentration for the emitter layer must be carefully studied. Emitter layer thickness is another important factor that affects sheet resistance and device performance. The effect of different doping concentrations on the device's sheet resistance and overall performance is shown in Table 3. Fig. 6 shows how the reduction in emitter doping affects short-circuit current and Voc. In this study, considering its low sheet resistance, a device with a thickness of 200  $\mu\text{m}$  and an emitter doping concentration of  $1 \times 10^{19} \text{ cm}^{-3}$  was identified as an ideal parameter. An emitter doping concentration of  $1 \times 10^{19} \text{ cm}^{-3}$  is chosen instead of  $1 \times 10^{18} \text{ cm}^{-3}$ , due to its considerable reduction in sheet resistance although the efficiency is decreased by less than 1%. By lowering the sheet resistance, the electrical performance and stability are enhanced generally.

**Table 3:** Influence of emitter layer doping concentration on device performance

Emitter Doping Concentration $\text{cm}^{-3}$	Short-circuit current (Isc), A	Maximum power output (Pmax), W	Open-circuit voltage (Voc), V	Fill Factor (FF)	Efficiency (%)
<b>Low to Medium Doping</b>					
$1 \times 10^{18}$	0.2671	0.1632	0.7265	0.8410	16.32
$2 \times 10^{18}$	0.267	0.1629	0.7247	0.8419	16.29
$3 \times 10^{18}$	0.267	0.1624	0.7225	0.8419	16.24
$4 \times 10^{18}$	0.2669	0.1619	0.7201	0.8424	16.19
$5 \times 10^{18}$	0.2668	0.1614	0.7175	0.8431	16.14
<b>Medium to High Doping</b>					
$1 \times 10^{19}$	0.2658	0.1583	0.7054	0.8443	15.83
$2 \times 10^{19}$	0.2621	0.1519	0.7054	0.6873	15.19
$3 \times 10^{19}$	0.2566	0.1458	0.6752	0.6873	14.58
$4 \times 10^{19}$	0.2499	0.1401	0.6668	0.6873	14.01
$5 \times 10^{19}$	0.2429	0.1347	0.6607	0.6873	13.47
<b>High Doping</b>					
$1 \times 10^{20}$	0.2145	0.1151	0.6469	0.6873	11.51
$2 \times 10^{20}$	0.191	0.1151	0.6417	0.6417	11.51
$3 \times 10^{20}$	0.1812	0.0969	0.6404	0.6417	9.69
$4 \times 10^{20}$	0.175	0.0931	0.6396	0.6417	9.31
$5 \times 10^{20}$	0.1702	0.0901	0.6389	0.6417	9.01

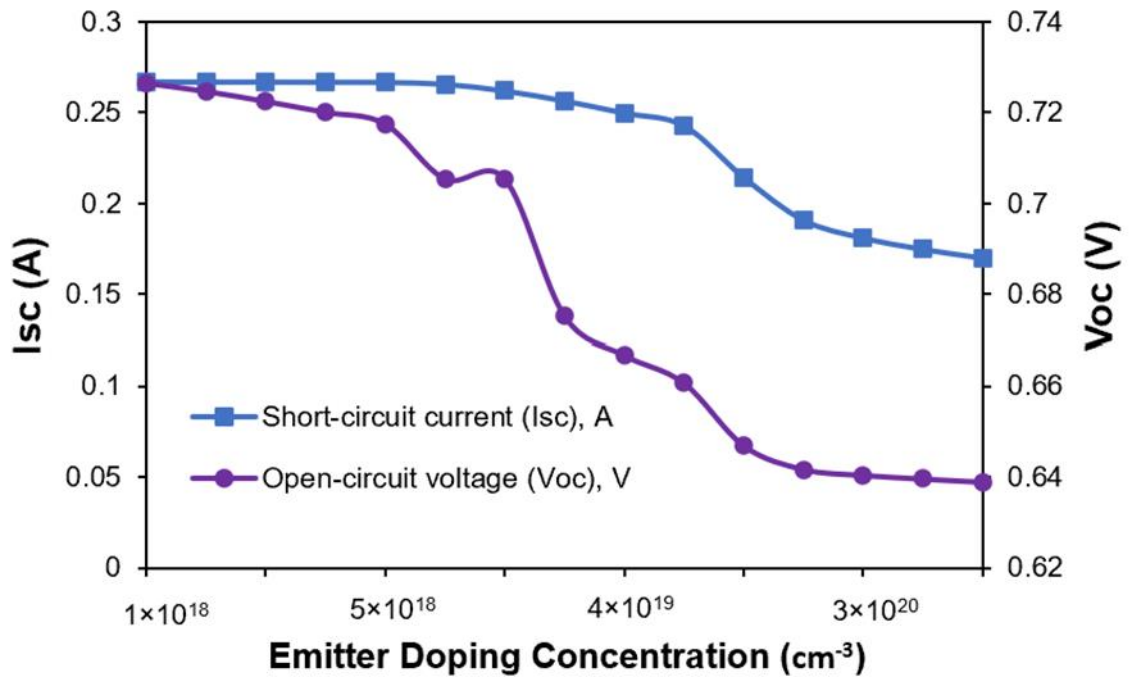
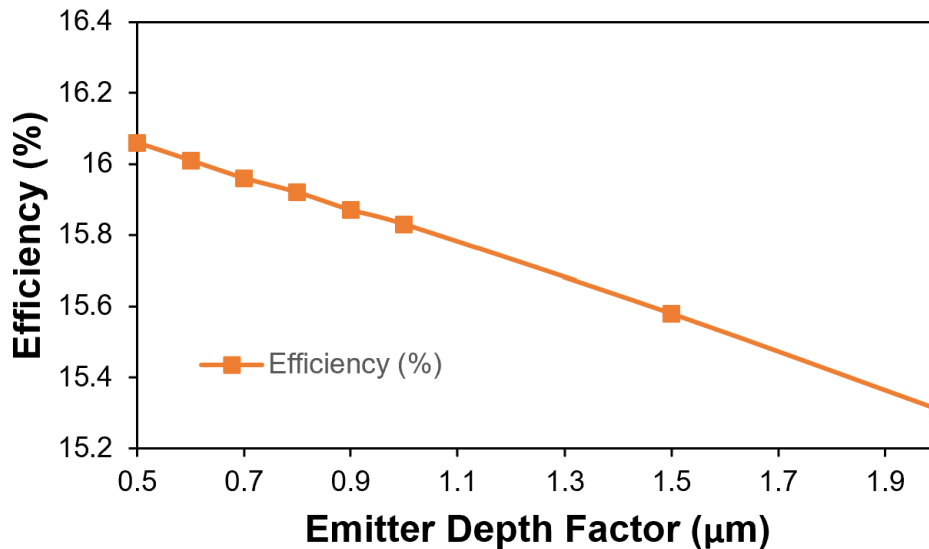


Figure 6: Effects of emitter doping concentration on Isc and Voc

The device's performance with different emitter thicknesses is displayed in Table 4. As the thickness of the emitter increases, the Isc and Voc both decrease. Although thick emitter layers have several disadvantages, lower emitter sheet resistance is preferred in a device. A thick, heavily doped emitter layer makes it difficult for light to get through, which reduces charge carrier generation and lowers device efficiency. Therefore, a high doping concentration of the emitter layer with a suitable thickness is needed. Fig. 7 shows the effects of the emitter depth layer on the efficiency of solar cells. The best efficiencies region is relatively broad with a junction depth ranging from 0.1 to 0.6 μm with a fixed doping concentration of emitter layer 1 × 10<sup>19</sup> cm<sup>-3</sup>. Here, 0.5 μm is considered the ideal thickness of the emitter layer. This depth provides the best overall efficiency and performance by striking a balance between minimizing recombination losses and maintaining low sheet resistance.

Table 4: Influence of emitter layer thickness on device performance

Emitter Depth Factor (μm)	Short-circuit current (Isc), A	Maximum power output (Pmax), W	Open-circuit voltage (Voc), V	Fill Factor (FF)	Efficiency (%)
0.1	0.2671	0.1627	0.7236	0.8418	16.27
0.2	0.267	0.1621	0.7205	0.8426	16.21
0.3	0.267	0.1616	0.7178	0.8432	16.16
0.4	0.2669	0.1611	0.7154	0.8437	16.11
0.5	0.2668	0.1606	0.7133	0.8439	16.06
0.6	0.2667	0.1601	0.7114	0.8438	16.01
0.7	0.2666	0.1596	0.7097	0.8435	15.96
0.8	0.2663	0.1592	0.7081	0.8443	15.92
0.9	0.2661	0.1587	0.7067	0.8439	15.87
1	0.2658	0.1583	0.7054	0.8443	15.83
1.5	0.2637	0.1558	0.7002	0.8438	15.58
2	0.2606	0.1531	0.6963	0.8437	15.31



**Figure 7:** Effects of the emitter depth layer on the efficiency of solar cells

*C. Effects of Back Surface Field (BSF) Concentration and Thickness on Device Performance*

A modern solar cell's back surface field (BSF), which is made up of a strongly doped layer at the cell's back, is an essential component. When a low-doped region meets a highly-doped region, an electric field is created that blocks minority mobile charge carriers and reduces recombination at the back layers of the solar cell [18]. Table 5 displays the outcomes of simulating how changing the amount of BSF doping affects the sheet resistance and the devices' general performance. Fig. 8 shows the effects of different concentrations of BSF doping on the overall performance of the device.

The highest measured efficiency is from solar cells with a BSF doping concentration of  $1 \times 10^{18} \text{ cm}^{-3}$ . From  $1 \times 10^{17}$  to  $1 \times 10^{18} \text{ cm}^{-3}$ , the open circuit voltage of the device is significantly affected by the doping concentration. However, after reaching a concentration of  $2 \times 10^{18} \text{ cm}^{-3}$ , the Voc reaches saturation and subsequently goes down gradually. The value of Isc also maintained at a doping concentration of  $1 \times 10^{18} \text{ cm}^{-3}$ , but it gradually falls as the doping concentrations go greater.

**Table 5:** Influence of BSF doping concentration on device performance

BSF Doping Concentration $\text{cm}^{-3}$	Short-circuit current (Isc), A	Maximum power output (Pmax), W	Open-circuit voltage (Voc), V	Fill Factor (FF)	Efficiency (%)
<b>Low to Medium Doping</b>					
$1 \times 10^{17}$	0.2668	0.1606	0.7134	0.8438	16.06
$2 \times 10^{17}$	0.2668	0.1606	0.7134	0.8438	16.06
$3 \times 10^{17}$	0.2668	0.1606	0.7134	0.8438	16.06
$4 \times 10^{17}$	0.2668	0.1606	0.7134	0.8438	16.06
$5 \times 10^{17}$	0.2668	0.1606	0.7134	0.8438	16.06
<b>Medium to High Doping</b>					
$1 \times 10^{18}$	0.2668	0.1606	0.7133	0.8439	16.06
$2 \times 10^{18}$	0.2668	0.1605	0.713	0.8437	16.05
$3 \times 10^{18}$	0.2668	0.1604	0.7125	0.8438	16.04
$4 \times 10^{18}$	0.2668	0.1603	0.712	0.8439	16.03
$5 \times 10^{18}$	0.2668	0.1602	0.7115	0.8439	16.02

**High Doping**

$1 \times 10^{19}$	0.2667	0.1594	0.7082	0.8439	15.94
$2 \times 10^{19}$	0.2664	0.1576	0.7008	0.8442	15.76
$3 \times 10^{19}$	0.266	0.1558	0.6939	0.8441	15.58
$4 \times 10^{19}$	0.2657	0.1541	0.6879	0.8431	15.41
$5 \times 10^{19}$	0.2653	0.1526	0.683	0.8422	15.26

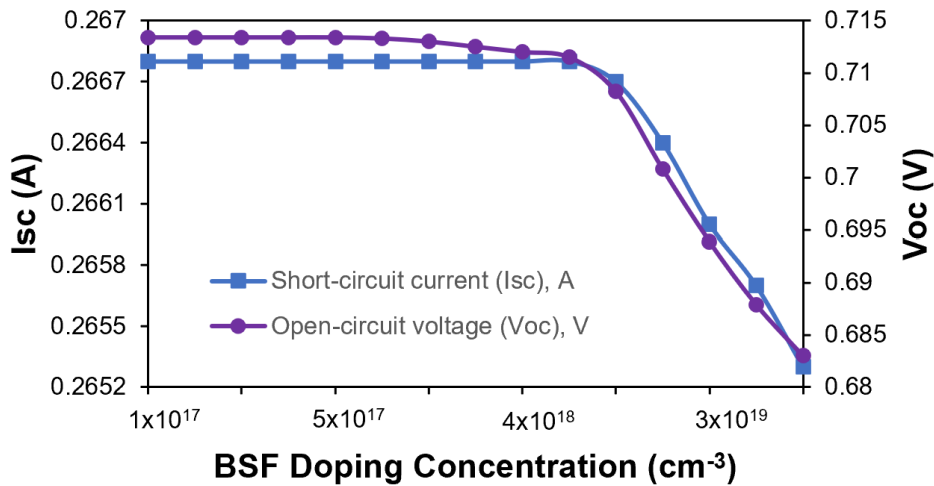


**Figure 8:** Effects of back surface field doping concentration on Isc and Voc

The BSF thickness also has an impact on overall efficiency as well. The efficiency decreases as the thickness of the BSF layer increases, as illustrated in Table 6. Lower values for Voc and Isc are observed when the BSF thickness increases. A thicker BSF may cause more recombination losses at the back surface, which in turn lowers Voc and Isc by decreasing the total number of effective charge carriers. In the contrary, when the thickness of the BSF layer increases, the fill factor (FF) rises. Figure 9 depicts how the thickness of the BSF layer affects solar cell efficiency. The efficiency of a solar cell is reduced when the BSF layer thickness increases because the increased recombination losses at the rear surface and the reduced effectiveness of the electric field lead to lower Isc and Voc. Although the fill factor may improve due to reduced series resistance, the overall efficiency decreases because the reductions in Isc and Voc have a more significant impact on the cell's performance. It is up to the individual solar cell design to decide between a range of 0.1 to 2 μm of BSF layer. If the primary goal is to maximize Voc and Isc while keeping manufacturing costs low, a 0.1 μm BSF layer is likely the best option. However, a 1 μm BSF layer could be chosen if achieving mechanical stability and increasing the fill factor are more important than slightly reducing Voc and Isc.

**Table 6:** Influence of BSF layer thickness on device performance

BSF Layer Depth Factor (μm)	Short-circuit current (Isc), A	Maximum power output (Pmax), W	Open-circuit voltage (Voc), V	Fill Factor (FF)	Efficiency (%)
0.1	0.2668	0.1606	0.7133	0.8439	16.06
0.2	0.2668	0.1606	0.7133	0.8439	16.06
0.3	0.2668	0.1606	0.7133	0.8439	16.06
0.4	0.2668	0.1606	0.7133	0.8439	16.06
0.5	0.2668	0.1606	0.7133	0.8439	16.06
0.6	0.2668	0.1606	0.7133	0.8439	16.06
0.7	0.2668	0.1606	0.7133	0.8439	16.06
0.8	0.2668	0.1606	0.7133	0.8439	16.06

0.9	0.2668	0.1606	0.7133	0.8439	16.06
1	0.2668	0.1606	0.7133	0.8439	16.06
1.5	0.2668	0.1606	0.7133	0.8439	16.06
2	0.2668	0.1606	0.7133	0.8439	16.06
5	0.2668	0.1605	0.7129	0.8438	16.05
10	0.2667	0.1604	0.7125	0.8441	16.04
15	0.2667	0.1604	0.7122	0.8445	16.04
20	0.2666	0.1603	0.7118	0.8447	16.03
25	0.2665	0.1602	0.7114	0.845	16.02
30	0.2665	0.1602	0.7111	0.8453	16.02
35	0.2664	0.1601	0.7108	0.8455	16.01
40	0.2663	0.16	0.7105	0.8456	16

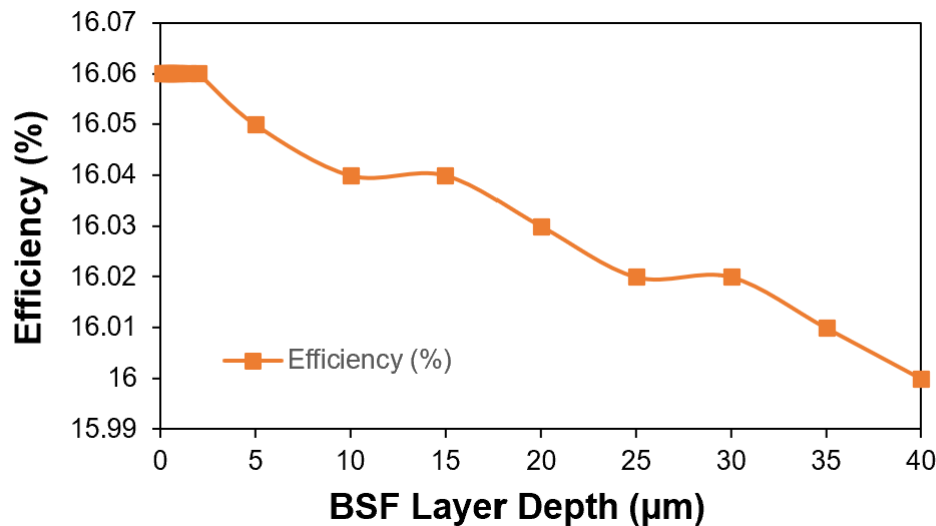


**Figure 9:** Effects of BSF layer thickness on efficiency of solar cells

*D. Effects of Antireflection Coating on Device Performance*

Another key component of efficient solar cells is the antireflection coating or ARC. ARC is a thin layer of dielectric material that is applied to the surface of solar cells to maximize transmission and decrease the total reflection of incoming light, hence producing more charge carriers [16]. The single, double, or multilayered dielectric materials with varying refractive indices that are stacked one after the other makeup ARCs, which are utilized in current solar cells. To learn how ARC impacts device performance, we modelled a variety of silicon surfaces, including those with no ARC applied, one layer of ARC, two layers of ARC, and three layers of ARC.

In Fig. 10, the single layer ARC (SLARC) is depicted using TiO<sub>2</sub> that is 67 nm thick and has a refractive index of 2.116. Fig. 11 depicts the double layer ARC (DLARC) that was constructed using materials with refractive indices of 1.39 and 2.371, along with thicknesses of 60.5 nm for zinc sulfide (ZnS) and 107 nm for magnesium fluoride (MgF<sub>2</sub>). The TLARC, depicted in Fig. 12, consisted of three layers: MgF<sub>2</sub>, silicon dioxide (SiO<sub>2</sub>), and TiO<sub>2</sub>. The layers' thicknesses were 80 nm, 30 nm, and 60 nm, and their refractive indices were 1.39, 1.48, and respectively 2.453. Table 7 shows the results of each device's performance.

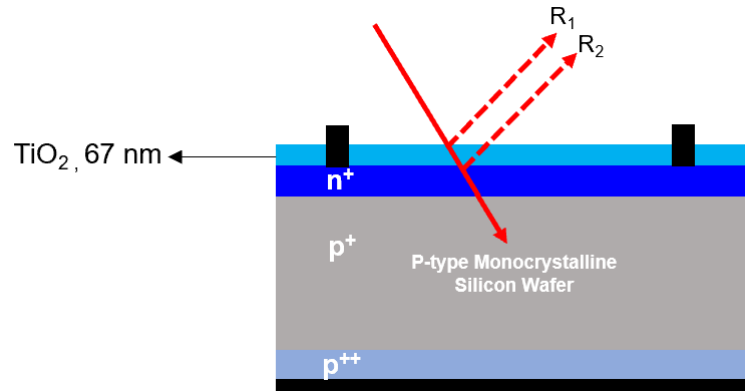


**Figure 10:** The single layer ARC (SLARC) on the standard structure of silicon solar cells

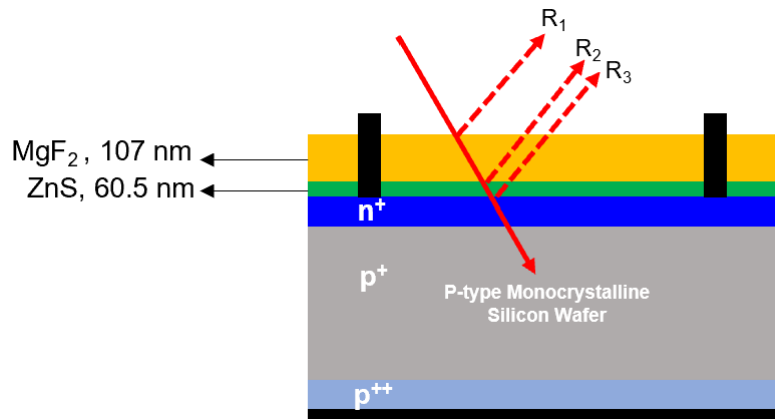


**Figure 11:** The double layer ARC (DLARC) on the standard structure of silicon solar cells

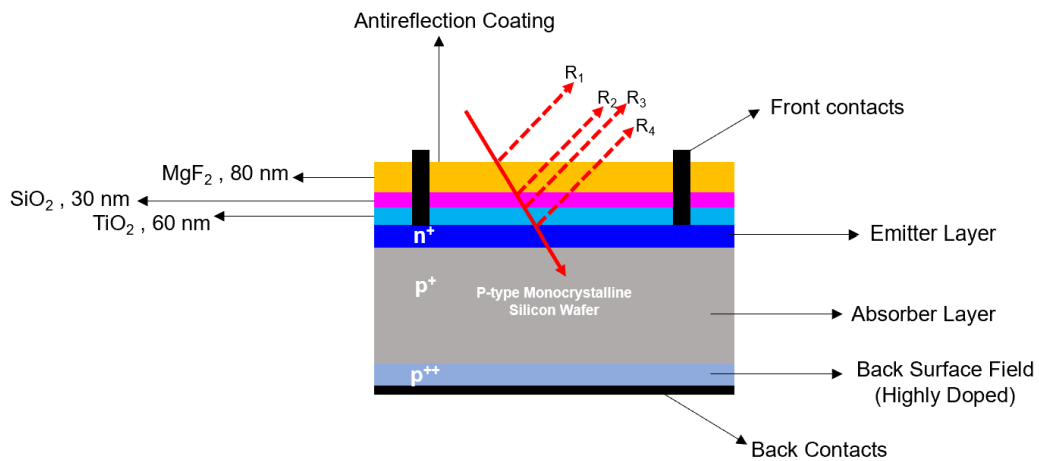


**Figure 12:** The triple layer ARC (TLARC) on the standard structure of silicon solar cells

**Table 7:** Device performance depends on the antireflection coating layer

ARC	Short-circuit current (Isc), A	Maximum power output (Pmax), W	Open-circuit voltage (Voc), V	Fill Factor (FF)	Efficiency (%)
None	0.2668	0.1606	0.7133	0.8439	16.06
SLARC	0.376	0.2298	0.7226	0.8458	22.98
DLARC	0.422	0.2447	0.7244	0.8005	24.47
TLARC	0.4227	0.2451	0.7245	0.8003	24.51

### E. Comparison of Optimal Simulated Solar Cell with a Fabricated Solar Cell

To make sure the simulation data was correct, measurements of a real solar cell in real-world settings were compared to those of a simulated device with the same parameters. Table 8 shows the electrical parameter comparison between the real solar cell and the simulation. One can see that the simulation results can predict the actual cell results in good agreement according to Table 8. In general, the results of the simulation were a little better than the parameters of the real cell. Due to lower recombination losses, the slightly better performance of the simulated cell is within a reasonable range. This shows that the simulation accurately predicted the cell's possible efficiency when resistive losses were taken into account.

**Table 8:** Optimal simulated solar cell electrical parameters compared to manufactured cell

Type	Short-circuit current (Isc), A	Maximum power output (Pmax), W	Open-circuit voltage (Voc), V	Fill Factor (FF)	Efficiency (%)
Actual Cell [51]	0.3909	0.2242	0.7250	0.7910	22.30
Simulated Cell (SLARC)	0.376	0.2298	0.7226	0.8458	22.98

## IV. CONCLUSIONS

In conclusion, this study shows how important it is to use PC1D simulation software to look at each device feature and find its best value to get the best conversion efficiency. Using simulation software is essential, but it's also important to think about device features like stability, durability, and how well the device handles extreme weather and constraints in the manufacturing process.

A solar cell made of monocrystalline silicon has been modelled using the PC1D programme. After checking their values against existing literature, we confirmed that all of the optimal solar cell parameters used in the simulation were acceptable. The PC1D simulation has thoroughly investigated all procedures using data collected from experiments. The most significant accomplishment was developing solar cell models that perform by more than 20% in efficiency. This was accomplished by meticulously analyzing an alternative approach and enhancing many aspects of the PC1D simulation. In real life, when solar cells are being made, adding the doping effect should make them at least 1% to 2% more efficient but it depends on the other parameters of the device. Using simulation before fabricating solar cells has other benefits, such as reducing engineering costs and better decision-making. It is advised to perform the solar cell simulation before manufacture to have a clear understanding of the parameters and how to adjust them to reduce expenses.

Lastly, this work demonstrates how crystalline silicon solar cell fabrication research and development could benefit from using simulation software like PC1D, thanks to its stability and accuracy.

## ACKNOWLEDGMENT

The authors would like to extend their gratitude to the Universiti Kebangsaan Malaysia. This project is funded under the Research University Grant (GUP) GUP-2022-015.

## REFERENCES

- [1] Z.A. Ghania, N. Aliyah Zainal Abidin & H. Othman, "Model Prototype of a Solar Tracking System Supplying Electrical Power for Sensors Used in a Natural Disaster Monitoring System", *Jurnal Kejuruteraan*, SI 6(2) 2023: 179 – 188. [https://doi.org/10.17576/jkukm-2023-si6\(2\)-19](https://doi.org/10.17576/jkukm-2023-si6(2)-19)
- [2] Fraunhofer Institute for Solar Energy Systems, ISE, "Photovoltaics Report", Freiburg, 17 May 2024.
- [3] Sawle, Yashwant, and M. Thirunavukkarasu. "Techno-economic comparative assessment of an off-grid hybrid renewable energy system for electrification of remote area." In *Design, analysis, and applications of renewable energy systems*, pp. 199-247. Academic Press, 2021. <https://doi.org/10.1016/B978-0-12-824555-2.00027-7>

- [4] Rabaia, Malek Kamal Hussien, Enas Taha Sayed, Mohammad Ali Abdelkareem, and Abdul Ghani Olabi. "Developments of Solar Photovoltaics." In Elsevier eBooks, 175–95, 2023. <https://doi.org/10.1016/b978-0-323-99568-9.00011-x>
- [5] Nurul Huda Abdul Razak, Kamaruzzaman Sopian, Nowshad Amin, and Md. Akhtaruzzaman "Investigation on the post-treatment after pulsed Nd:YAG laser texturing on silicon solar cells surfaces", Proc. SPIE 11387, Energy Harvesting and Storage: Materials, Devices, and Applications X, 1138717 (18 May 2020). <https://doi.org/10.1117/12.2572780>
- [6] N. H. A. Razak, K. Sopian, N. Amin and M. Akhtaruzzaman, "An Investigation of Optical Absorption of Pulsed Nd:YAG Laser Texturing on Silicon Solar Cells Surfaces Before and After Post Treatment," 2020 IEEE International Conference on Semiconductor Electronics (ICSE), Kuala Lumpur, Malaysia, 2020, pp. 116-119.  
<https://doi.org/10.1109/icse49846.2020.9166871>
- [7] N. H. A. Razak, K. Sopian, N. Amin and M. Akhtaruzzaman, "Reducing Reflectance on Silicon Solar Cells Surfaces by Controlling X-Y Translation Table Speeds of Pulsed Nd:YAG Laser System," 2020 47th IEEE Photovoltaic Specialists Conference (PVSC), Calgary, AB, Canada, 2020, pp. 2109-2112. <https://doi.org/10.1109/pvsc45281.2020.9300959>
- [8] Nurul Huda Abdul Razak, Nowshad Amin, Kazi Sajedur Rahman, Jagadeesh Pasupuleti, Md. Akhtaruzzaman, Kamaruzzaman Sopian, Munirah D. Albaqami, Ammar Mohamed Tighezza, Zeid A. Alothman, Mika Sillanpää, "Influence of pulsed Nd:YAG laser oscillation energy on silicon wafer texturing for enhanced absorption in photovoltaic cells", Results in Physics, Volume 48, 2023, 106435. <https://doi.org/10.1016/j.rinp.2023.106435>
- [9] Nd: YAG Laser Texturization on Silicon Surface, Razak, Nurul Huda Abdul, and Nowshad Amin. "Nd:YAG Laser Texturization on Silicon Surface." Advanced Materials Research. Trans Tech Publications, Ltd., February 2014. <https://doi.org/10.4028/www.scientific.net/amr.894.201>
- [10] Nabil, Amira, Ahmed Shaker, Mohamed Abouelatta, Hani Ragai, and Christian Gontrand. "Tunneling FET Calibration Issues: Sentaurus vs. Silvaco TCAD." In Journal of Physics: Conference Series, vol. 1710, no. 1, p. 012003. IOP Publishing, 2020. <https://doi.org/10.1088/1742-6596/1710/1/012003>
- [11] Liu, Huan, Shiyu Qu, Lei Zhao, and Wenjing Wang. "Optimization of heterojunction back-contact (HBC) crystalline silicon solar cell based on Quokka simulation." Materials Today Communications 36 (2023): 106816. <https://doi.org/10.2139/ssrn.4491670>
- [12] Rodriguez, John W., Naomi Nandakumar, and Shubham Duttagupta. "'SolarEYE' loss analysis of screen-printed, n-type silicon solar cells with 'monoPoly'PECVD rear passivated contacts." Solar Energy Materials and Solar Cells 223 (2021): 110961. <https://doi.org/10.1016/j.solmat.2021.110961>
- [13] Siraj, Saba, Sofia Tahir, Adnan Ali, Nasir Amin, Khalid Mahmood, and Alina Manzoor. "Assessing the impact of front grid metallization pattern on the performance of BSF silicon solar cells." Silicon 13 (2021): 4237-4245. <https://doi.org/10.1007/s12633-021-01235-9>
- [14] Metin, Bengul, Nese Kavasoglu, and A. Sertap Kavasoglu. "AFORS-HET simulation for investigating the performance of ZnO/n-CdS/p-CdTe/Ag solar cell depending on CdTe acceptor concentration and temperature." Physica B: Condensed Matter 649 (2023): 414504. <https://doi.org/10.1016/j.physb.2022.414504>
- [15] Shwan, Yadgar Hussein, and Berun Nasraddin Ghafoor. "Study the Effect of Doping and Thickness on IV characteristic of Silicon Solar Cells Using PC1D Simulation." Tikrit Journal of Pure Science 29, no. 1 (2024): 128-135. <https://doi.org/10.25130/tjps.v29i1.1520>
- [16] Meenakshi, S., and S. Baskar. "Design of multi-junction solar cells using PC1D." In 2013 International Conference on Energy Efficient Technologies for Sustainability, pp. 443-449. IEEE, 2013.  
<https://doi.org/10.1109/iceets.2013.6533424>

- [17] Chowdhury, Ahrar Ahmed, and Abasifreke Ebong. "A simulation model for optimizing the performance of bifacial Si solar cells." In 2015 12th International Conference on High-capacity Optical Networks and Enabling/Emerging Technologies (HONET), pp. 1-4. IEEE, 2015. <https://doi.org/10.1109/honet.2015.7395439>
- [18] Belarbi, Moussaab, Abdellah Benyoucef, and Boumediene Benyoucef. "Simulation of the solar cells with PC1D, application to cells based on silicon." *Advanced Energy: An International Journal (AEIJ)* 1, no. 3 (2014).
- [19] Jiang, Chuan, Tian Ze Li, Xia Zhang, and Luan Hou. "Simulation of Silicon Solar Cell Using PC1D." *Advanced Materials Research* 383–390 (November 2011): 7032–36. <https://doi.org/10.4028/www.scientific.net/amr.383-390.7032>
- [20] MANDONG, Al-montazer, and Ü. Z. Ü. M. Abdullah. "Analysis of silicon solar cell device parameters using PC1D." *Sakarya University Journal of Science* 23, no. 6 (2019): 1190-1197. <https://doi.org/10.16984/saufenbilder.557490>
- [21] Hashmi, Galib, Abdur Rafique Akand, Mahbulul Hoq, and Habibur Rahman. "Study of the enhancement of the efficiency of the monocrystalline silicon solar cell by optimizing effective parameters using PC1D simulation." *Silicon* 10 (2018): 1653-1660. <https://doi.org/10.1007/s12633-017-9649-3>
- [22] Chiao, Shu-Chung, Jiu-Lin Zhou, and H. A. Macleod. "Optimized design of an antireflection coating for textured silicon solar cells." *Applied Optics* 32, no. 28 (1993): 5557-5560. <https://doi.org/10.1364/oic.1992.pd1>
- [23] Manikandan, A. V. M., and Shanthi Prince. "Electrical performance analysis and optimization of monofacial and bifacial crystalline silicon solar cells." *Optica Applicata* 53, no. 3 (2023). <https://doi.org/10.37190/oa230301>
- [24] Al-sultan, Moatasem AM, and Serra Altınoluk. "ON THE PERFORMANCE LIMITS FOR MONO CRYSTALLINE SILICON SOLAR CELLS: A COMPARATIVE STUDY." *Mugla Journal of Science and Technology* 8, no. 2 (2022): 82-89. <https://doi.org/10.22531/muglajsci.1101048>
- [25] Sahu, Mohnish Kumar, Naman Shukla, and Sanjay Tiwari. "Study of the Enhanced Efficiency of Crystalline Silicon Solar Cells by Optimizing Anti Reflecting Coating using PC1D Simulation." *Journal of Ravishankar University* 35, no. 2 (2022): 1-7. <https://doi.org/10.52228/jrub.2023-35-2-1>
- [26] Fathi, M., A. Aissat, and M. Ayad. "Design of Building Integrated Photovoltaic (BIPV) and integration of photons converters." *Energy Procedia* 18 (2012): 377-383. <https://doi.org/10.1016/j.egypro.2012.05.049>
- [27] Muhfidin, Rivan, and Song Yu. "Temperature Effects on the Performance of Silicon Solar Cells using PC1D." In *Proceedings of the 2nd International Conference on Industrial and Technology and Information Design, ICITID 2021, 30 August 2021, Yogyakarta, Indonesia. 2021.* <https://doi.org/10.4108/eai.30-8-2021.2311501>
- [28] Book, Felix, Amir Dastgheib-Shirazi, Bernd Raabe, Helge Haverkamp, Giso Hahn, and Peter Grabitz. "Detailed analysis of high sheet resistance emitters for selectively doped silicon solar cells." (2009). <https://doi.org/10.4229/24thEUPVSEC2009-2CV.5.3>
- [29] Sadhukhan, Sourav, Shiladitya Acharya, Tamalika Panda, Nabin Chandra Mandal, Sukanta Bose, Anupam Nandi, Gourab Das et al. "Evolution of high efficiency passivated emitter and rear contact (PERC) solar cells." In *Sustainable Developments by Artificial Intelligence and Machine Learning for Renewable Energies*, pp. 63-129. Elsevier, 2022. <https://doi.org/10.1016/b978-0-323-91228-0.00007-0>
- [30] Thirunavukkarasu, Gokul Sidarth, Mehdi Seyedmahmoudian, Jaideep Chandran, Alex Stojcevski, Maruthamuthu Subramanian, Raj Marnadu, S. Alfaify, and Mohd Shkir. "Optimization of mono-crystalline silicon solar cell devices using PC1D simulation." *Energies* 14, no. 16 (2021): 4986. <https://doi.org/10.3390/en14164986>
- [31] Subramanian, Maruthamuthu, Omar M. Aldossary, Manawwer Alam, Mohd Ubaidullah, Sreedevi Gedi, Lakshminarayanan Vaduganathan, Gokul Sidarth Thirunavukkarasu et al. "Optimization of Antireflection

- Coating Design Using PC 1 D Simulation for c-Si Solar Cell Application." *Electronics* 10, no. 24 (2021): 3132. <https://doi.org/10.3390/electronics10243132>
- [32] Baig, Hasan, Hiroyuki Kanda, Abdullah M. Asiri, Mohammad Khaja Nazeeruddin, and Tapas Mallick. "Increasing efficiency of perovskite solar cells using low concentrating photovoltaic systems." *Sustainable Energy & Fuels* 4, no. 2 (2020): 528-537. <https://doi.org/10.1039/c9se00550a>
- [33] Bunea, Gabriela E., Karen E. Wilson, Yevgeny Meydbray, Matthew P. Campbell, and Denis M. De Ceuster. "Low light performance of mono-crystalline silicon solar cells." In *2006 IEEE 4th World Conference on Photovoltaic Energy Conference*, vol. 2, pp. 1312-1314. IEEE, 2006. <https://doi.org/10.1109/wcpec.2006.279655>
- [34] Polman, Albert, Mark Knight, Erik C. Garnett, Bruno Ehrler, and Wim C. Sinke. "Photovoltaic materials: Present efficiencies and future challenges." *Science* 352, no. 6283 (2016): aad4424. <https://doi.org/10.1126/science.aad4424>
- [35] Um, Han-Don, Inchan Hwang, Deokjae Choi, and Kwanyong Seo. "Flexible crystalline-silicon photovoltaics: light management with surface structures." *Accounts of Materials Research* 2, no. 9 (2021): 701-713. <https://doi.org/10.1021/accountsmr.1c00038>
- [36] Hallam, Brett J., Phill G. Hamer, Alison M. Ciesla née Wenham, Catherine E. Chan, Bruno Vicari Stefani, and Stuart Wenham. "Development of advanced hydrogenation processes for silicon solar cells via an improved understanding of the behavior of hydrogen in silicon." *Progress in Photovoltaics: Research and Applications* 28, no. 12 (2020): 1217-1238. <https://doi.org/10.1002/pip.3240>
- [37] Ho, Wen-Jeng, Shih-Ya Su, Yi-Yu Lee, Hong-Jhang Syu, and Ching-Fuh Lin. "Performance-enhanced textured silicon solar cells based on plasmonic light scattering using silver and indium nanoparticles." *Materials* 8, no. 10 (2015): 6668-6676. <https://doi.org/10.3390/ma8105330>
- [38] Ribeyron, Pierre-Jean. "Crystalline silicon solar cells: Better than ever." *Nature Energy* 2, no. 5 (2017): 1-2. <https://doi.org/10.1038/nenergy.2017.67>
- [39] Di Sabatino, Marisa, Rania Hendawi, and Alfredo Sanchez Garcia. "Silicon Solar Cells: Trends, Manufacturing Challenges, and AI Perspectives." *Crystals* 14, no. 2 (2024): 167. <https://doi.org/10.3390/cryst14020167>
- [40] Lim, Jong Rok, Sihan Kim, Hyung-Keun Ahn, Hee-Eun Song, and Gi Hwan Kang. "Analysis of the bowing phenomenon for thin c-Si solar cells using partially processed c-Si solar cells." *Energies* 12, no. 9 (2019): 1593. <https://doi.org/10.3390/en12091593>
- [41] Depauw, Valérie, Christos Trompoukis, Inès Massiot, Wanghua Chen, Alexandre Dmitriev, Pere Roca i Cabarrocas, Ivan Gordon, and Jef Poortmans. "Sunlight-thin nanophotonic monocrystalline silicon solar cells." *Nano Futures* 1, no. 2 (2017): 021001. <https://doi.org/10.1088/2399-1984/aa7d7c>
- [42] Elfiky, Shymaa Sabry, Aref Eliwa, Mohamed Zahran, Ahmed Kassem, and Ahmed Farghal. "A Study on the Impact of PN-Junction Doping Concentration on the Efficiency of Monocrystalline Silicon Solar Cells." *Sohag Engineering Journal* 3, no. 2 (2023): 165-177. <https://doi.org/10.21608/sej.2023.224272.1041>
- [43] Alimardani, Ali, Ebrahim Asl-Soleimani, and Ali Afzali-Kusha. "SIMULATION AND OPTIMIZATION OF EMITTER DEPTH AND DOPING FOR SILICON SOLAR CELLS UNDER CONCENTRATED SUNLIGHT." <https://doi.org/10.18086/swc.2011.03.02>
- [44] Lu, Xuesong, Ruiying Hao, Martin Diaz, Robert L. Opila, and Allen Barnett. "Improving GaP solar cell performance by passivating the surface using Al<sub>x</sub>Ga<sub>1-x</sub>P epi-layer." *IEEE Journal of the Electron Devices Society* 1, no. 5 (2013): 111-116. <https://doi.org/10.1109/jeds.2013.2266410>

- [45] Ahmed, M. S., S. M. Ahmad, and M. Subhyaljader. "STUDY THE ROLE OF EFFECTIVE PARAMETERS IN ENHANCEMENT OF THE SILICON SOLAR CELL PERFORMANCE USING PC1D SIMULATION." *Journal of Ovonic Research* 16, no. 2 (2020). <https://doi.org/10.15251/jor.2020.161.97>
- [46] Mularso, Kelvian Tirtakusuma. "Analysis of back surface field (BSF) performance in P-type and N-type monocrystalline silicon wafer." In *E3S Web of Conferences*, vol. 43, p. 01006. EDP Sciences, 2018. <https://doi.org/10.1051/e3sconf/20184301006>
- [47] Saif, Ala'eddin A., and Bandar Alamri. "Efficiency Enhancement Using an Extra BSF Layer in Single-Layer GaAs Solar Cell." In *International Conference on Materials Engineering and Nanotechnology*, pp. 54-64. Singapore: Springer Nature Singapore, 2023. [https://doi.org/10.1007/978-981-97-4080-2\\_5](https://doi.org/10.1007/978-981-97-4080-2_5)
- [48] Rahman, Md Ferdous, Mithun Chowdhury, Latha Marasamy, Mustafa KA Mohammed, Md Dulal Haque, Sheikh Rashel Al Ahmed, Ahmad Irfan, Aijaz Rasool Chaudhry, and Souraya Goumri-Said. "Improving the efficiency of a CIGS solar cell to above 31% with Sb 2 S 3 as a new BSF: a numerical simulation approach by SCAPS-1D." *RSC advances* 14, no. 3 (2024): 1924-1938. <https://doi.org/10.1039/d3ra07893k>
- [49] Suzuki, Akio, Minoru Kaneiwa, Tatsuo Saga, and Sumio Matsuda. "Progress and future view of silicon space solar cells in Japan." *IEEE Transactions on electron devices* 46, no. 10 (1999): 2126-2132. <https://doi.org/10.1109/16.792007>
- [50] Chen, Ke, Rui Wu, Hongmei Zheng, Yuanyuan Wang, and Xiaopeng Yu. "Enhanced light trapping in thin-film silicon solar cells with concave quadratic bottom gratings." *Applied optics* 57, no. 19 (2018): 5348-5355. <https://doi.org/10.1364/ao.57.005348>
- [51] Tsunomura, Yasufumi, Yukihiro Yoshimine, Mikio Taguchi, Toshiaki Baba, Toshihiro Kinoshita, Hiroshi Kanno, Hitoshi Sakata, Eiji Maruyama, and Makoto Tanaka. "Twenty-two percent efficiency HIT solar cell." *Solar Energy Materials and Solar Cells* 93, no. 6-7 (2009): 670-673. <https://doi.org/10.1016/j.solmat.2008.02.037>